



Removal of arsenic from acid wastewater via sulfide precipitation and its hydrothermal mineralization stabilization

Bin HU^{1,2}, Tian-zu YANG^{1,2}, Wei-feng LIU^{1,2}, Du-chao ZHANG^{1,2}, Lin CHEN^{1,2}

1. School of Metallurgy and Environment, Central South University, Changsha 410083, China;

2. National Engineering Laboratory for High Efficiency Recovery of Refractory Nonferrous Metals, Changsha 410083, China

Received 14 February 2019; accepted 26 August 2019

Abstract: To achieve a safe treatment of arsenic-containing acid wastewater, a new process was proposed, including arsenic removal via sulfide precipitation and hydrothermal mineralization stabilization. Under optimal conditions of sulfide precipitation, 99.65% of arsenic from wastewater was precipitated in the form of amorphous As_2S_3 . The As leaching concentration of amorphous As_2S_3 in TCLP (toxicity characteristic leaching procedure) test was up to 212.97 mg/L, therefore, hydrothermal mineralization was adopted to improve the stability of amorphous As_2S_3 . The results showed that the As leaching concentration of mineralized As_2S_3 was only 4.82 mg/L. Furthermore, the amorphous As_2S_3 could be transformed into crystallized As_2S_3 (orpiment) in the presence of mineralizer Na_2SO_4 . Simultaneously, the As leaching concentration of crystallized As_2S_3 was further reduced to 3.86 mg/L. Hydrothermal mineralization was an effective method for the stabilization of As_2S_3 . Therefore, this process has a greater application in the treatment of arsenic-containing wastewater.

Key words: arsenic-containing wastewater; arsenic removal; stabilization; sulfide precipitation; hydrothermal mineralization; hydrothermal crystallization

1 Introduction

In pyrometallurgy process, the smelting of heavy metals sulfide concentrates bearing arsenic introduces large amounts of arsenic into the off-gas and dust [1,2], which contain a particularly high concentration of arsenic and toxic heavy metals [3]. Then, arsenic-containing wastewater was mainly produced during the scrubbing process of off-gas and separation process of arsenic from dust [4,5]. The concentration of arsenic in wastewater occasionally ranges from 0.5 to 20 g/L [6]. It is widely known that arsenic occurring in the water system poses a significant threat to the human health and ecological system, even at low concentrations [7,8]. Therefore, the removal and stabilization of arsenic from smelting wastewater have become an urgent issue for environmental protection departments and smelting plants [9].

Currently, there are several methods available to

remove arsenic from wastewater, such as precipitation, adsorption, reverse osmosis, ion-exchange, and membrane filtration [10]. Of these methods, precipitation is the most effective method for the treatment of wastewater with high arsenic content [11]. Arsenic can be removed in the form of calcium arsenate, ferric arsenate, or sulfides. However, calcium arsenates could react with CO_2 and release arsenic into the environment when they are exposed to the atmosphere [12,13]. Ferric arsenate is also unstable [14,15], even though its removal efficiency is high. Sulfide precipitation has been widely employed to remove arsenic by adding sulfides owing to the rapid reaction rates and good dewatering characteristics of sulfides [16–18]. Moreover, the As content of arsenic sulfides is significantly higher than that of the other forms, which favors the volume reduction of arsenic solidification/stabilization residues.

However, arsenic sulfides obtained during the reaction process are not suitable for direct land filling due to the unsatisfactory results of the TCLP test.

Foundation item: Projects (2018YFC1901601, 2018YFC1901604, 2018YFC1901605) supported by the National Key Research and Development Program of China; Project (201806375047) supported by the Visiting Scholar of China Scholarship Council; Project (51404296) supported by the Young Scientists Fund of the National Natural Science Foundation of China

Corresponding author: Wei-feng LIU; Tel: +86-13548654403; E-mail: liuweifeng@csu.edu.cn

DOI: 10.1016/S1003-6326(19)65147-2

Therefore, solidification/stabilization technology is employed to treat the precipitates obtained from precipitation process. The encapsulated stabilization and mineralization are two types of arsenic stabilization methods that have been widely investigated in recent years. Encapsulated stabilization processes include inorganic gelation material encapsulation, organic gelation material encapsulation, and melting stabilization [19]. Of various methods to treat arsenic waste, Portland cement stabilization appears to be the most acceptable method due to its advantages like simplicity, efficiency, and low cost [20]. However, this technology has been limited due to its poor durability, high As leaching rate in the long term, and a large volume of solidified mass. Hence, mineralization has been proposed to treat arsenic waste pollution, which is a highly individualized approach to industrial wastewater containing arsenic. A variety of minerals, such as scorodite ($\text{FeAsO}_4 \cdot 2\text{H}_2\text{O}$) [21,22], tooeleite ($\text{Fe}_6(\text{AsO}_3)_4(\text{SO}_4)(\text{OH})_4 \cdot 4\text{H}_2\text{O}$) [23,24] and arsenical natroalunite [25,26], have been proved to be capable of solidifying arsenic and removing it from wastewater. However, scorodite should be cautiously adopted due to its tendency to dissolve incongruently in water [27,28]. Both tooeleite and arsenical natroalunite have limitations, such as low arsenic content, high volume, and high synthesis cost, which limit their application in the solidification/stabilization process. Therefore, more research should be carried out to increase the arsenic content of the solidified mass and reduce its volume.

According to the geochemistry of arsenic, arsenic mainly contains in minerals such as orpiment (As_2S_3), realgar (AsS) and arsenopyrite (FeAsS) in the earth [29]. It can be informed that arsenic exhibits strong affinity with sulfur and iron. And the sulphophile affinity would

be beneficial to hydrothermal transformation of arsenic sulfide precipitates to orpiment or realgar. Therefore, a new process for the removal and stabilization of arsenic from acid wastewater via sulfide precipitation–hydrothermal crystallization was proposed. Arsenic precipitated in the form of As_2S_3 by adding Na_2S . The resulting sulfide precipitate, reductant, and mineralizer were mixed with water. Subsequently, hydrothermal experiments were carried out in an autoclave. The optimal conditions were systematically investigated. The stabilized mass was characterized by XRD and SEM–EDS. Finally, the short-term stability was evaluated by the TCLP (toxicity characteristic leaching procedure).

2 Experimental

2.1 Materials

The arsenic-containing wastewater used in this study was prepared through the selective precipitation of Cu from copper smelting waste acid, which was sourced from the Henan Yuguang Gold and Lead Group Co., Ltd., China. The initial pH of arsenic-containing wastewater was 0.6. The main chemical composition of the arsenic-containing wastewater is shown in Table 1.

Table 1 Concentrations of main elements in arsenic-containing wastewater (mg/L)

As (III)	As (V)	Sb	Pb	Cd	Fe	Na
12562.0	Trace	48.63	1.5	12.6	84.2	1853.8

2.2 Experimental procedures

A flow chart representing the process is shown in Fig. 1. The sulfide precipitation experiments were

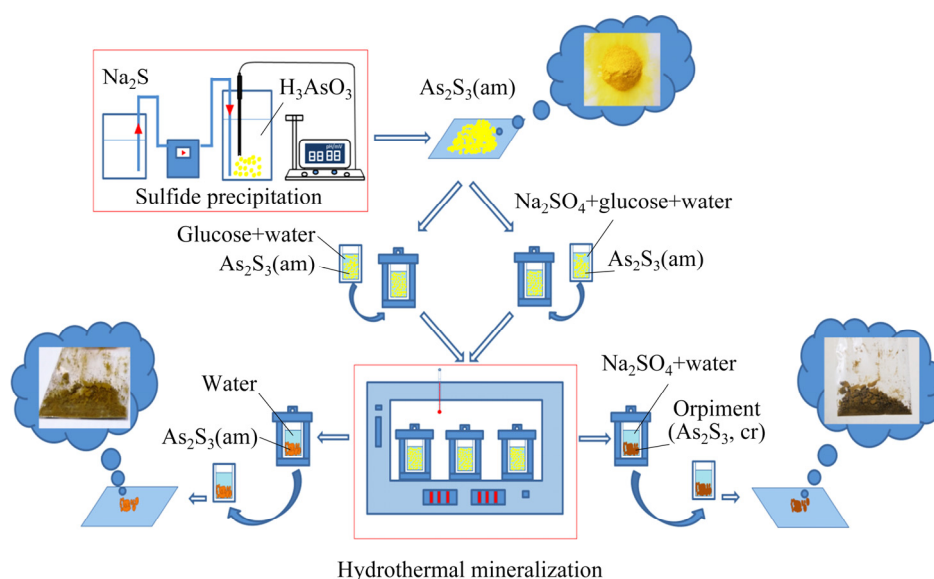


Fig. 1 Flow chart of removal of arsenic from acid wastewater via sulfide precipitation and its hydrothermal mineralization stabilization

performed in a 400 mL flask, which was equipped with a magnetic stirrer. The flask was placed in a thermostatic water bath and the temperature was controlled accurately within ± 0.5 °C. The Na_2S solution (110 g/L) was added to the arsenic-containing wastewater using a constant-flow pump when the temperature reached the pre-set value. The terminal pH was determined and continuously monitored by a pH meter with a combination electrode. The pH of the slurry was adjusted with dilute H_2SO_4 to a desired pH when the Na_2S solution began to add until the experiment finished. The effects of terminal pH, S^{2-}/As molar ratio, temperature, and reaction time on the precipitation efficiency of As were investigated. After completing the experiment, the slurry was filtered and washed. And the sulfide precipitates were dried and weighed for characterization and next step.

For hydrothermal mineralization, the arsenic sulfide precipitates of 2.0 g and a certain amount of the glucose were mixed with deionized water or Na_2SO_4 solution. And the filling rate of autoclave was adjusted by regulating the volume of deionized water or Na_2SO_4 solution. Subsequently, the hydrothermal mineralization of amorphous As_2S_3 was performed in an autoclave. The hydrothermal treatment was carried out by placing the vessels in a dry oven for 6–24 h at a given temperature in the range of 160–240 °C. After the hydrothermal treatment, the vessels were cooled down in atmospheric air. The precipitates were filtered and desiccated. Finally, the short-term stability of precipitates was evaluated through the TCLP test. The effects of hydrothermal mineralization temperature, filling rate, glucose/precipitate mass ratio, hydrothermal duration, and mineralizer concentration on the As leaching concentration of stabilized mass were investigated.

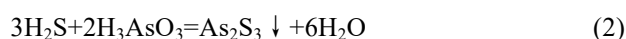
2.3 Analytical methods

The compositions of the filtrates and the dried precipitates were determined by an inductively coupled plasma–atomic emission spectrometry (Thermo, ICP–AES Agilent 7500, USA). The dried precipitates were pulverized in a mortar and characterized using a scanning electron microscope (Jeol, SEM JSM–6360LV, Japan), equipped with a spectrometer for microanalysis based on an energy dispersive X-ray spectroscopy system (EDAX, EDS GENESIS 60S, USA). Phase identification and particle size distribution of the samples were carried out using an X-ray diffraction instrument (Rigaku, XRD TTRAX–3, Japan) and a laser particle size analyzer (Mastersizer, MS2000, UK), respectively. The specific surface area and pore volume were determined by a porosity analyzer (Quantachrome, QuadraSorb SI, USA). The pH values of wastewater and slurry were determined using a pH meter (Mettler Toledo, 320–SpH, Switzerland) with a combination electrode.

3 Results and discussion

3.1 Sulfide precipitation of As

Sulfide reactions, involving those of S^{2-} with metal ions (Cu^{2+} , Cd^{2+} , and Fe^{2+}) and H_3AsO_3 , occur via the addition of a sulfide agent (Na_2S solution) into the arsenic-containing wastewater. The solubility product constants of As_2S_3 , CdS , and FeS are 2.1×10^{-22} , 8.0×10^{-27} , and 6.3×10^{-18} , respectively. Therefore, the above mentioned elements could precipitate completely when the dosage of Na_2S was sufficient. The main reactions that occur during the sulfide precipitation process are as follows:



3.1.1 Effect of terminal pH

The effect of terminal pH on the precipitation efficiency of As was investigated at 25 °C for 120 min, with S^{2-}/As molar ratios of 1.5:1, 2.0:1, and 2.5:1 (Fig. 2). As shown in Fig. 2, when the terminal pH of the arsenic-containing wastewater increased from 1.0 to 5.0 with different S^{2-}/As molar ratios, the As precipitation efficiency remained constant within 120 min. However, the precipitation efficiency of As reduced sharply when the terminal pH of the arsenic-containing wastewater increased up to 6.0. Moreover, the reducing rangeability of the As precipitation efficiency increased when the S^{2-}/As molar ratios increased. The main side-reactions with the change in pH during the sulfide precipitation process are as follows:

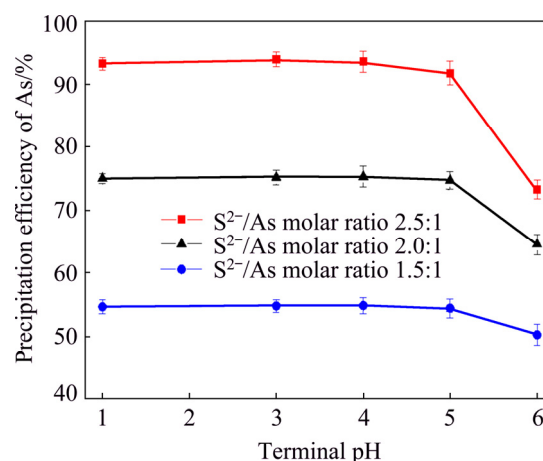
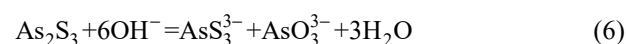


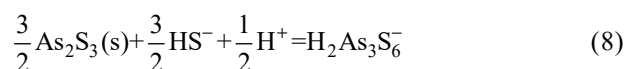
Fig. 2 Effect of terminal pH on As precipitation efficiency in arsenic-containing wastewater



This indicates that a high pH value would result in the re-dissolution of As_2S_3 precipitate (Eqs. (5) and (6)) [30,31]. Moreover, the use of a solution with a low pH value will result in the emission of H_2S gas (Eq. (7)) [32]. Therefore, the terminal pH should be 4.0.

3.1.2 Effect of S^{2-}/As molar ratio

The effect of S^{2-}/As molar ratio on the precipitation efficiency of As was investigated at 25 °C for 120 min, with terminal pH values of 4.0 and 5.0 (Fig. 3). At terminal pH values of 4.0 and 5.0, the precipitation efficiencies of As were up to 99.1% and 97.2%, respectively, with the increase in S^{2-}/As molar ratio from 1.5:1 to 3.0:1. With further increase in the S^{2-}/As molar ratio, the precipitation efficiency of As remained constant at a terminal pH of 4.0. However, at a terminal pH of 5.0, the precipitation efficiency of As experienced a slight reduction when the S^{2-}/As molar ratio further increased. This can be attributed to the dissolution of As_2S_3 with increasing S^{2-} , which occurs as follows [31]:



Therefore, at a terminal pH of 4.0, the optimal S^{2-}/As molar ratio should be 3.0:1.

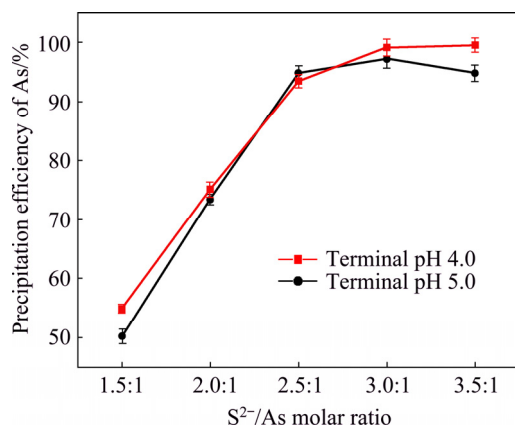


Fig. 3 Effect of S^{2-}/As molar ratio on As precipitation efficiency in arsenic-containing wastewater

3.1.3 Effect of reaction temperature

The effect of reaction temperature on the precipitation efficiency of As was investigated at a S^{2-}/As molar ratio of 3.0:1 for 120 min, with a terminal pH of 4.0 (Fig. 4). The results showed that the precipitation efficiency of As was barely influenced by the reaction temperature. When the temperature increased from 25 to 85 °C, no difference was observed in the precipitation efficiency of As. Therefore, the reaction temperature should be 25 °C.

3.1.4 Effect of reaction time

The effect of reaction time on the precipitation efficiency of As was investigated at a S^{2-}/As molar ratio

of 3.0:1, 25 °C, with a terminal pH of 4.0 (Fig. 5). As shown in Fig. 5, the precipitation efficiency of As increased sharply when the reaction time was increased from 30 to 60 min. With further increase in the reaction time, the precipitation efficiency of As remained constant. This can be attributed to the slow flow rate of Na_2S solution. The flow rate of the Na_2S solution was set to be 1 mL/min, which prevented the emission of H_2S , while significantly increasing the reaction time required to add the Na_2S solution. Therefore, the appropriate reaction time is 60 min.

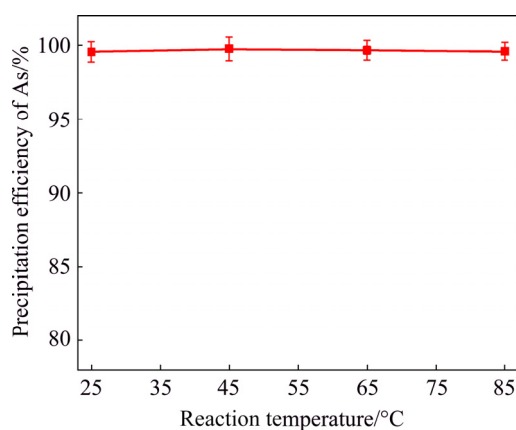


Fig. 4 Effect of reaction temperature on As precipitation efficiency in arsenic-containing wastewater

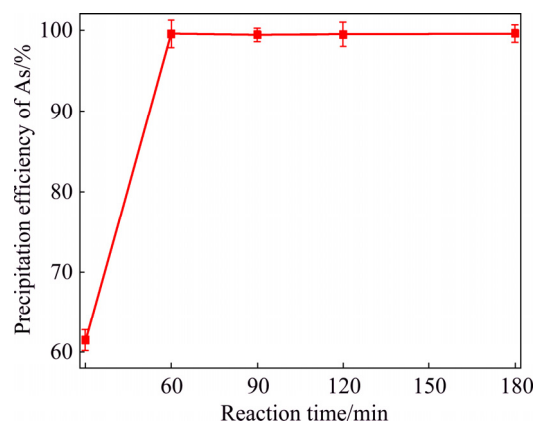


Fig. 5 Effect of reaction time on As precipitation efficiency in arsenic-containing wastewater

3.1.5 Optimal experiment

According to the above experiments, the optimal conditions for sulfide precipitation of arsenic were obtained as follows: terminal pH of 4.0, S^{2-}/As molar ratio of 3.0:1, reaction temperature of 25 °C, and reaction time of 60 min. Under the optimal conditions, the As concentration in the As-removed wastewater is 6.72 mg/L, which indicates an As precipitation efficiency of up to 99.65% (Table 2). The As and S contents of the precipitate are 59.19% and 36.87% at the S/As molar ratio is 1.45:1 (Table 3). This means that the formula of the sulfide precipitate is As_2S_3 .

Table 2 Concentrations of main elements in As-removed wastewater (mg/L)

As	S	Sb	Na	Fe	Cd	Pb
6.72	14326	1.82	4028.57	3.47	0.95	0.81

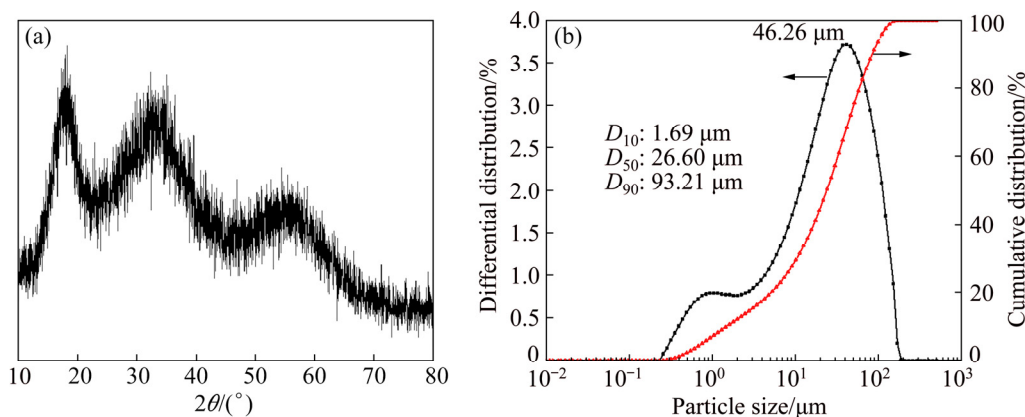
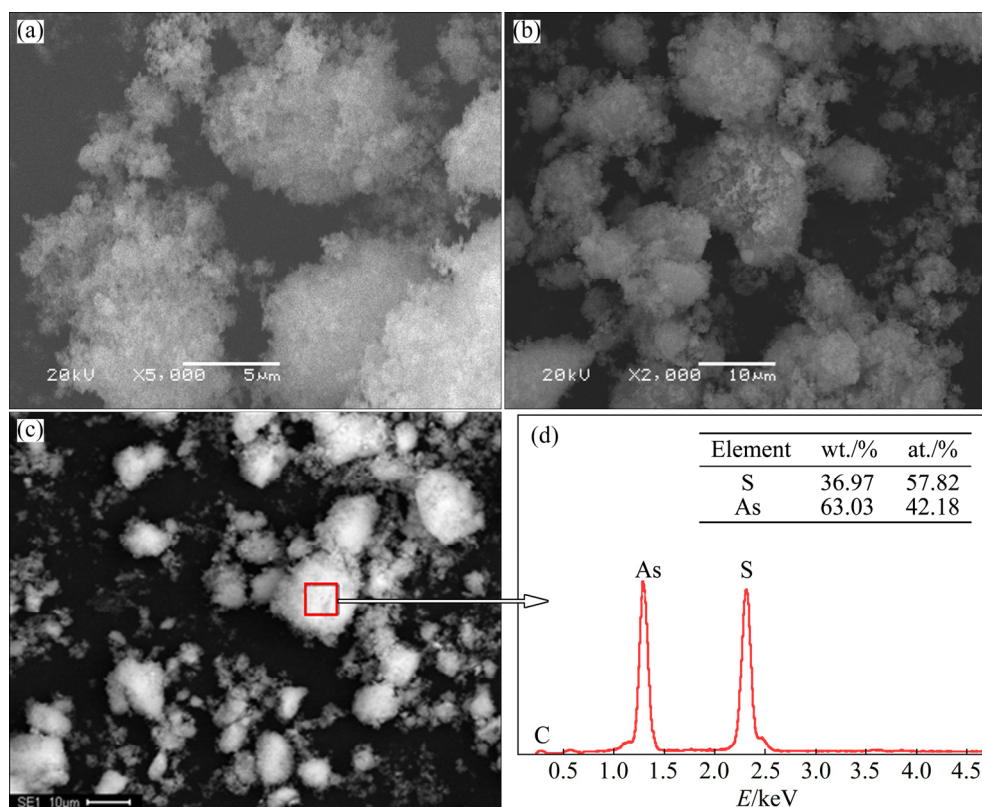
Table 3 Chemical composition of sulfide precipitate (wt.%)

As	S	Sb	Na	Fe	Cd	Pb	Others
59.19	36.87	0.4	0.75	0.41	0.05	0.05	2.28

The sulfide precipitate was also characterized using XRD, particle size distribution, and SEM–EDS. The XRD pattern of sulfide precipitate does not have any sharp diffraction peaks that can be indexed to As_2S_3

crystals (Fig. 6(a)), which illustrates that the precipitate is amorphous. The results of the particle size distribution are presented in Fig. 6(b). The particles sizes range widely from 0.286 to 169.46 μm . Most particles are distributed in the size range of 41.52–51.55 μm . The surface weighted mean D [3,2] of 4.92 μm illustrates that the sulfide precipitate has a large specific surface area (BET: 33.55 m^2/g).

SEM images of the sulfide precipitate are shown in Figs. 7(a) and (b). The flocculent particles of the precipitate are attached to the surface of large particles and the precipitate morphology exhibits the agglomeration of incompact fine particles. The porous structure of the sulfide precipitate results in more

**Fig. 6** XRD pattern (a) and particle size distribution (b) of sulfide precipitate obtained during sulfide precipitation**Fig. 7** SEM (a, b), BSE (c) images and EDS pattern (d) of sulfide precipitate obtained through sulfide precipitation

exposure of As to air or water (pore volume: 0.15 mL/g). Thus, the arsenic sulfide particles present high chemical activity due to the surface effect. A toxicity leaching test for arsenic sulfide precipitate was performed. The As leaching concentration was up to 212.97 mg/L, which exceeded the limit of 5.0 mg/L. Therefore, arsenic sulfide precipitates should be classified as hazardous wastes.

3.2 Hydrothermal mineralization of As_2S_3

The TCLP test results show that arsenic sulfide precipitates obtained through the sulfidation process are not appropriate for direct land filling due to their high leaching toxicity and weak stability, which may be caused by the characteristics of amorphous structures, such as small particle size, large specific surface area, and loose structure. As is well known, most precipitates generated through the sulfide precipitation are amorphous owing to the rapid reaction rate. Therefore, to simulate the epithermal metallogenic conditions of arsenic sulfide, the hydrothermal mineralization process was adopted to achieve the mineralization and stabilization of arsenic. To obtain the optimal conditions for the hydrothermal mineralization of the sulfide precipitate, the effects of hydrothermal temperature, filling rate, glucose mass fraction (relative to precipitate), and hydrothermal duration of the process on the As leaching concentration of the mineralized As_2S_3 in the TCLP test were investigated.

3.2.1 Effect of hydrothermal temperature

In the hydrothermal process, high pressure and high temperature are important factors, which are closely related to crystal formation and its structural variation. Changes in temperature inevitably result in the variation of water vapor pressure in the autoclave [33]. Therefore, the effect of hydrothermal temperature on the As concentration of mineralized As_2S_3 in the TCLP test was initially investigated with filling rate of 60% and glucose mass fraction of 0 for 12 h (Fig. 8).

When the hydrothermal temperature increased from 160 to 240 °C, the As leaching concentration of the mineralized As_2S_3 reduced gradually. The tendency illustrated that high temperature was beneficial to the mineralization of amorphous As_2S_3 . However, hydrothermal temperature was largely determined by the material properties of the autoclave, such as heat resistance and pressure resistance. Considering the safety of autoclave experiments and the hydrothermal mineralization result, the hydrothermal temperature should be 240 °C.

3.2.2 Effect of filling rate

The filling rate of the autoclave is another factor affecting the hydrothermal pressure. Higher pressure was obtained due to higher filling rate, compared to a lower

filling rate at the same temperature. However, exorbitant pressure would destroy the inner vessel of the autoclave, as well as threaten personnel safety. Usually, filling rates of 50%–80% are reasonable. Therefore, the appropriate filling rate was determined through experimental study with glucose mass fraction of 0, at 200 and 240 °C for 12 h, respectively.

As shown in Fig. 9, the As leaching concentration of mineralized As_2S_3 in the TCLP test was barely influenced by the filling rate. When the filling rate increased from 50% to 80% at 200 °C, no obvious changes were observed in the concentration of As. Similar results were observed when the filling rate increased from 50% to 70% at 240 °C. However, the inner vessel burst when the filling rate was increased up to 80% at 240 °C. In short, the filling rate has negligible effect on the stability of mineralized As_2S_3 . Therefore, a filling rate of 70% is appropriate in the hydrothermal process.

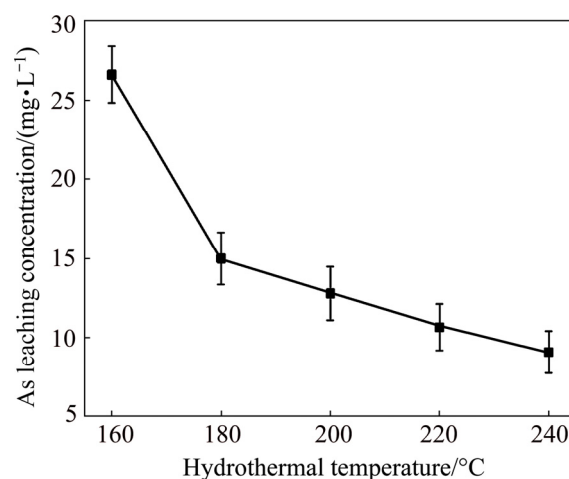


Fig. 8 Effect of hydrothermal temperature on As leaching concentration of mineralized As_2S_3

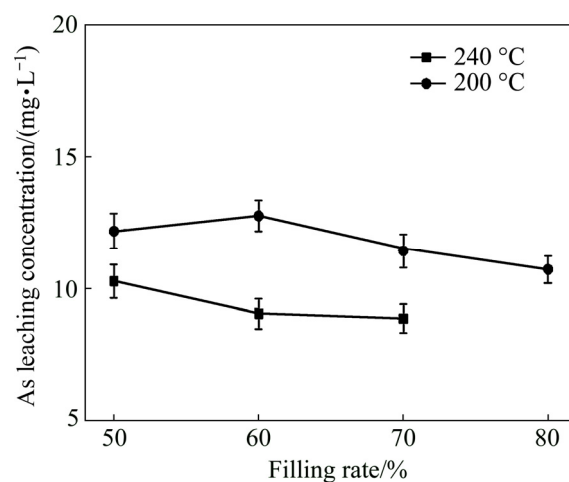


Fig. 9 Effect of filling rate on As leaching concentration of mineralized As_2S_3

3.2.3 Effect of glucose mass fraction

Owing to the high chemical activity of the arsenic sulfide precipitate, the dissolution of As_2S_3 would be enhanced in the presence of O_2 [34]. Therefore, glucose was added as a reductant in the hydrothermal mineralization process to avoid the oxidation and dissolution of As_2S_3 . Figure 10 illustrates the effect of the glucose mass fraction on the As leaching concentration of mineralized As_2S_3 in the TCLP test with filling rate of 70%, at 240 °C for 12 h.

As seen in Fig. 10, the As leaching concentration of mineralized As_2S_3 reduced with the addition of glucose from 0 to 5.0%. However, there was an obvious increase in the As leaching concentration of mineralized As_2S_3 when the glucose mass fraction increased from 5.0% to 25.0%. This meant that the higher glucose mass fraction reduced the stability of mineralized As_2S_3 . This could be attributed to the decomposition of glucose in the hydrothermal system, which may break the compact structure of mineralized As_2S_3 . Therefore, a glucose mass fraction of 5.0% was sufficient for the hydrothermal mineralization of As_2S_3 .

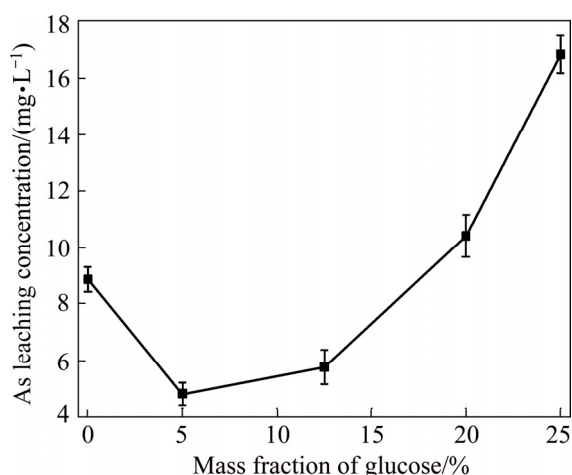


Fig. 10 Effect of glucose mass fraction on As leaching concentration of mineralized As_2S_3

3.2.4 Effect of hydrothermal duration

The effect of hydrothermal duration on the As leaching concentration of mineralized As_2S_3 in the TCLP test was investigated at 240 °C, glucose mass fraction of 5.0%, and filling rate of 70% (Fig. 11). The As leaching concentration of mineralized As_2S_3 exhibited an obvious reduction by prolonging the hydrothermal duration from 6 to 12 h. When the hydrothermal duration was increased further, the As leaching concentration of mineralized As_2S_3 in the TCLP test remained constant. Therefore, 12 h is sufficient for enhancing the stability of mineralized As_2S_3 via the hydrothermal process.

3.2.5 Optimal experiment

From the above experiments, the optimal conditions

were determined as follows: temperature of 240 °C, filling rate of 70%, glucose mass fraction of 5.0%, and hydrothermal duration of 12 h.

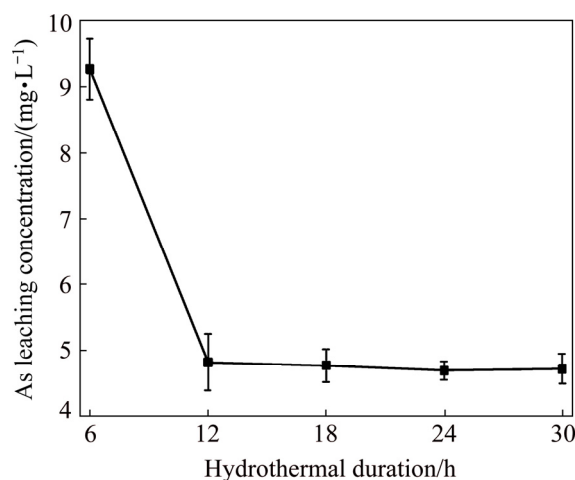


Fig. 11 Effect of hydrothermal duration on As leaching concentration of mineralized As_2S_3

The mineralized As_2S_3 was also characterized using XRD and SEM. The XRD pattern of the hydrothermal precipitate is shown in Fig. 12, which illustrates that the mineralized As_2S_3 continued to be amorphous. SEM analysis of the sulfide precipitate is shown in Fig. 13. Compared to the SEM images of the sulfide precipitate (Figs. 7(a, b)), there were no small, dispersed particles. Instead, in Fig. 13, smooth, compact particles aggregated tightly into coral-like particles. Several coral-like particles were cross-linked to each other to form a larger reticular structure. The specific surface area and pore volume of mineralized As_2S_3 were 2.93 m²/g and 0.005 mL/g, respectively. The change in morphology of arsenic sulfide residue eliminated the small size effect and improved the stability. The As leaching concentration of mineralized As_2S_3 in the TCLP test was 4.82 mg/L, which was lower than the limit of 5.0 mg/L.

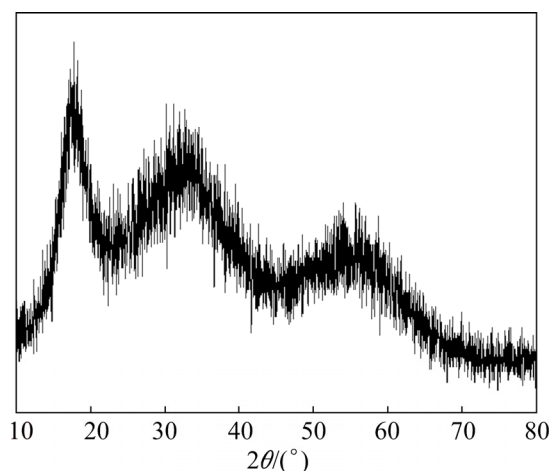


Fig. 12 XRD pattern of mineralized As_2S_3

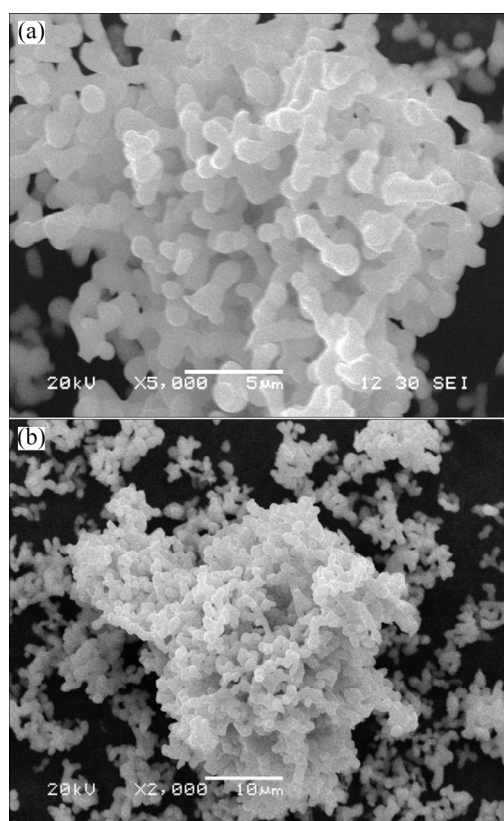


Fig. 13 SEM images of mineralized As_2S_3 : (a) Higher magnification; (b) Lower magnification

3.3 Hydrothermal crystallization of As_2S_3

Hydrothermal process is an important method for synthesizing crystals. Temperature, pressure, and mineralizer are significant factors impacting the crystallinity and morphology. However, the as-prepared As_2S_3 under the above hydrothermal conditions was still amorphous. In arsenic geochemistry, an orpiment mineral was formed in epithermal and mesothermal hydrothermal systems in temperature range between 100 and 350 °C [35]. The highest temperature under our laboratory conditions, 240 °C, was favorable for the formation of arsenic sulfide crystals. Therefore, the absence of a mineralizer could be the reason for the as-prepared As_2S_3 to be amorphous.

Mineralizers are compounds such as salts, acids, or alkalis with a low melting point, whose solubility increases with increasing temperature. The addition of a mineralizer can improve the solubility of the solute in a hydrothermal solution, as well as significantly decrease the viscosity of the solution, thus increasing the mobility of the components in the system [36]. Moreover, the stability, crystal morphology, and structure of hydrothermal products change when different mineralizers are used [37]. Owing to the strong acidity of arsenic-containing wastewater, NaOH was used to adjust the pH, which resulted in the formation of Na_2SO_4 . To

promote the reutilization of Na_2SO_4 and reduce the cost, Na_2SO_4 was employed as the mineralizer in the hydrothermal crystallization process. Therefore, the effect of the Na_2SO_4 content on the As leaching concentration of crystallized As_2S_3 was investigated under the optimal conditions of hydrothermal mineralization.

From the experimental study, the As leaching concentration of crystallized As_2S_3 in the TCLP test was slightly influenced by the Na_2SO_4 content under the optimal conditions of hydrothermal mineralization (Fig. 14). The As leaching concentration reduced from 4.82 to 3.86 mg/L when the Na_2SO_4 content increased from 0 to 6 wt.%. However, obvious changes in the crystallization of the as-prepared As_2S_3 were observed in the XRD test, as shown in Fig. 15. There were no obvious peaks in the XRD images without the mineralizer (Fig. 15(a)), which illustrates that the mineralized As_2S_3 was amorphous. With the increase in the Na_2SO_4 content, the intensities of the diffraction

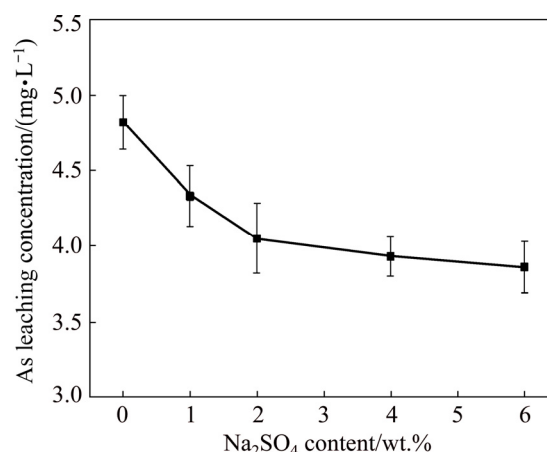


Fig. 14 Effect of Na_2SO_4 content on As leaching concentration of crystallized As_2S_3

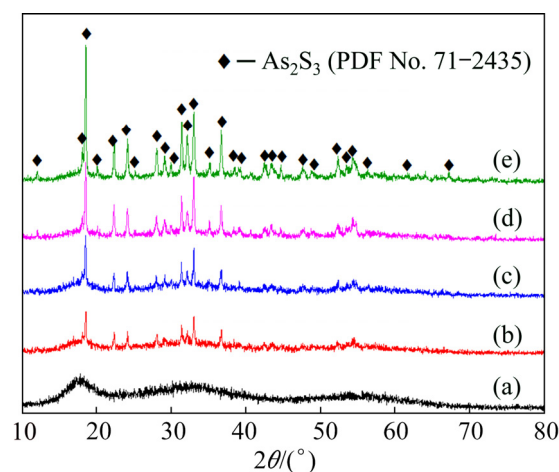


Fig. 15 XRD patterns of crystallized As_2S_3 at different Na_2SO_4 contents: (a) 0 wt.%; (b) 1 wt.%; (c) 2 wt.%; (d) 4 wt.%; (e) 6 wt.%

peaks of crystallized As_2S_3 (orpiment, PDF No. 71–2435) were strengthened. When the of Na_2SO_4 content was 6 wt.%, the crystallinity of As_2S_3 was significantly better than that of the others. SEM images of the as-prepared As_2S_3 (with 6 wt.% Na_2SO_4) revealed that the small flocculent particles (Figs. 7(a, b)) were transformed into large polygonal bulks (Figs. 16(a, b)), which were different in morphologies from the mineralized As_2S_3 (Figs. 13(a, b)). Therefore, Na_2SO_4 content of 6 wt.% was appropriate.

Under the optimal conditions, the As and S contents of the crystallized As_2S_3 were 58.54 wt.% and 35.43 wt.%, respectively, and the S/As molar ratio was 1.42:1, which was close to the theoretical S/As molar ratio of 1.5:1 (Table 4). BSE image and EDS pattern are shown respectively in Figs. 16(c, d) for reference. The specific surface area of $1.63 \text{ m}^2/\text{g}$ and pore volume of 0.006 mL/g also illustrated that the flocculent particles of the sulfide precipitate aggregated into compact crystal particles under hydrothermal conditions, which favored the reduction of As leaching concentration. The changes in SEM images and XRD patterns illustrated that the presence of Na_2SO_4 was favorable for the recrystallization of amorphous As_2S_3 .

Table 4 Chemical composition of crystallized As_2S_3 (wt.%)

As	S	Sb	Na	Fe	Cd	Pb	Others
58.54	35.43	0.5	3.2	0.48	0.09	0.08	1.68

4 Conclusions

(1) In sulfide precipitation process, 99.65% of As was precipitated in the form of amorphous As_2S_3 under the conditions of terminal pH of 4.0, S^{2-}/As molar ratio of 3.0:1, reaction temperature of 25°C , and reaction time of 60 min. The As leaching concentration of amorphous As_2S_3 in the TCLP test was up to 212.97 mg/L , which was significantly higher than the limit of 5.0 mg/L . Therefore, the arsenic sulfide precipitate should be classified as a hazardous waste.

(2) In hydrothermal mineralization process, the stability of As_2S_3 was obviously improved under the optimal conditions of hydrothermal temperature of 240°C , filling rate of 70%, glucose mass fraction of 5%, and hydrothermal duration of 12 h. The As leaching concentration of mineralized As_2S_3 in the TCLP test can be reduced to 4.82 mg/L . However, the mineralized As_2S_3 continued to be amorphous.

(3) In hydrothermal crystallization process, the As leaching concentration of the as-prepared As_2S_3 was reduced to 3.86 mg/L when 6 wt.% Na_2SO_4 was added as a mineralizer. The XRD results showed that the as-prepared As_2S_3 was crystallized As_2S_3 (orpiment, PDF No. 71–2435). Therefore, orpiment can be an alternative mineral for the stabilization of arsenic from wastewater due to the high arsenic content, low volume, and satisfactory stability.

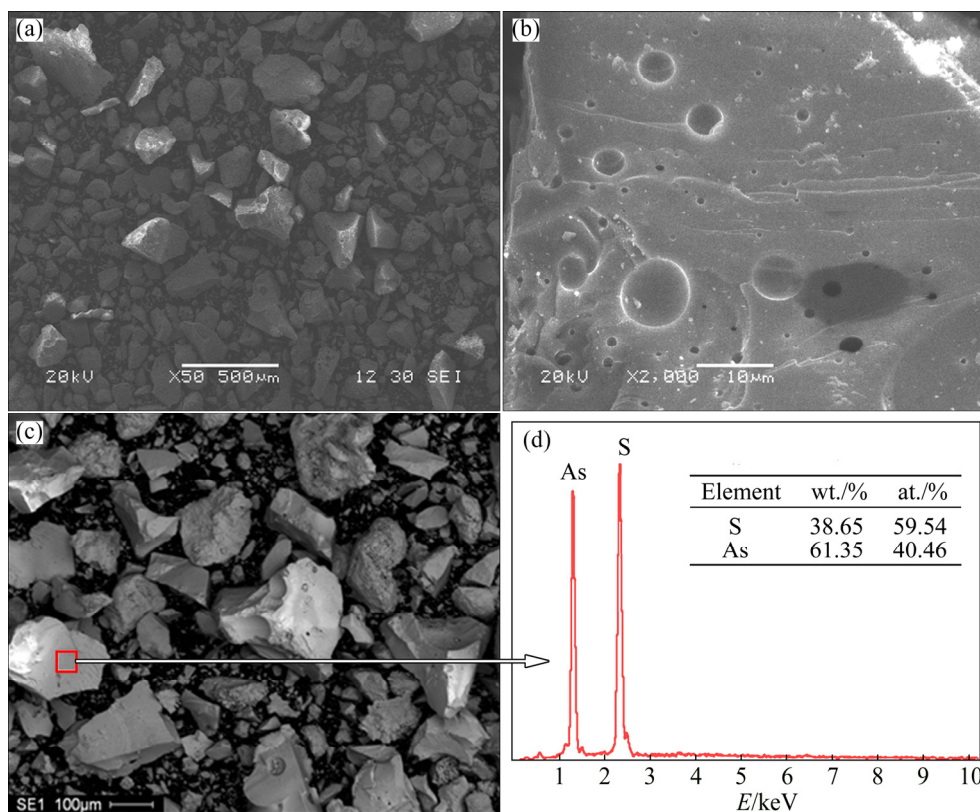


Fig. 16 SEM (a, b), BSE (c) images, and EDS pattern (d) of crystallized As_2S_3

References

- [1] HENAO D M O, GODOY M A M. Jarosite pseudomorph formation from arsenopyrite oxidation using *Acidithiobacillus ferrooxidans* [J]. Hydrometallurgy, 2010, 104: 162–168.
- [2] CHAI Li-yuan, SHI Mei-qing, LIANG Yan-jie, TANG Jing-wen, LI Qing-zhu. Behavior, distribution and environmental influence of arsenic in a typical lead smelter [J]. Journal of Central South University, 2015, 22(4): 1276–1286.
- [3] JIANG Guo-min, PENG Bing, CHAI Li-yuan, WANG Qing-wei, SHI Mei-qing, WANG Yun-yan, LIU Hui. Cascade sulfidation and separation of copper and arsenic from acidic wastewater via gas–liquid reaction [J]. Transactions of Nonferrous Metals Society of China, 2017, 27: 925–931.
- [4] YANG Kang, LIU Wei, ZHANG Tian-fu, YAO Li-wei, QIN Wen-qing. Water leaching of arsenic trioxide from metallurgical dust with emphasis on its kinetics [J]. Journal of Central South University, 2019, 26(9): 2328–2339.
- [5] MCHUGH L F, BALLIETT R, MOZOLIC J A. The sulfide ore looping oxidation process: An alternative to current roasting and smelting practice [J]. JOM, 2008, 60(7): 84–87.
- [6] DU Ying, LU Qiong, CHEN Hui-yun, DU Ya-guang, DU Dong-yun. A novel strategy for arsenic removal from dirty acid wastewater via $\text{CaCO}_3\text{-Ca(OH)}_2\text{-Fe(III)}$ processing [J]. Journal of Water Process Engineering, 2016, 12: 41–46.
- [7] IAKOVLEVA E, MAYDANNIK P, IVANOVA T V, SILLANPÄÄ M, TANG W Z, MÄKILÄ E, SALONEN J, GUBAL A, GANEEV A A, KAMWILAIKAK K, WANG S. Modified and unmodified low-cost iron-containing solid wastes as adsorbents for efficient removal of As(III) and As(V) from mine water [J]. Journal of Cleaner Production, 2016, 133: 1095–1104.
- [8] KITCHIN K T. Recent advances in arsenic carcinogenesis: Modes of action, animal model systems, and methylated arsenic metabolites [J]. Toxicology & Applied Pharmacology, 2001, 172: 249–261.
- [9] YANG Jin-qin, CHAI Li-yuan, LI Qing-zhu, SHU Yu-de. Redox behavior and chemical species of arsenic in acidic aqueous system [J]. Transactions of Nonferrous Metals Society of China, 2017, 27: 2063–2072.
- [10] KARTINEN E O, MARTIN C J. An overview of arsenic removal processes [J]. Desalination, 1995, 103: 79–88.
- [11] LEIST M, CASEY R J, CARIDI D. The management of arsenic wastes: Problems and prospects [J]. Journal of Hazardous Materials, 2000, 76: 125–138.
- [12] NISHIMURA T, ROBINS R G. A re-evaluation of the solubility and stability regions of calcium arsenites and calcium arsenates in aqueous solution at 25 °C [J]. Mineral Processing & Extractive Metallurgy Review, 1998, 18: 283–308.
- [13] PENG Bing, LEI Jie, MIN Xiao-bo, CHAI Li-yuan, LIANG Yan-jie, YOU Yang. Physicochemical properties of arsenic-bearing lime–ferrate sludge and its leaching behaviors [J]. Transactions of Nonferrous Metals Society of China, 2017, 27: 1188–1198.
- [14] FUJITA T, TAGUCHI R, ABUMIYA M, MATSUMOTO M, SHIBATA E, NAKAMURA T. Novel atmospheric scorodite synthesis by oxidation of ferrous sulfate solution: Part I [J]. Hydrometallurgy, 2008, 90: 92–102.
- [15] KRAUSE E, ETTTEL V A. Solubilities and stabilities of ferric arsenate compounds [J]. Hydrometallurgy, 1989, 22: 311–337.
- [16] NAZARI A M, RADZINSKI R, GHAREMAN A. Review of arsenic metallurgy: Treatment of arsenical minerals and the immobilization of arsenic [J]. Hydrometallurgy, 2017, 174: 258–281.
- [17] LIU Rui-ping, YANG Zhong-chao, HE Zi-liang, WU Li-yuan, HU Cheng-zhi, WU Wen-zhu, QU Jiu-hui. Treatment of strongly acidic wastewater with high arsenic concentrations by ferrous sulfide (FeS): Inhibitive effects of S(0)-enriched surfaces [J]. Chemical Engineering Journal, 2016, 304: 986–992.
- [18] LEWIS A E. Review of metal sulphide precipitation [J]. Hydrometallurgy, 2010, 104: 222–234.
- [19] SINGH T S, PANT K K. Solidification/stabilization of arsenic containing solid wastes using Portland cement, fly ash and polymeric materials [J]. Journal of Hazardous Materials, 2006, 131: 29–36.
- [20] KUNDU S, GUPTA A K. Immobilization and leaching characteristics of arsenic from cement and/or lime solidified/stabilized spent adsorbent containing arsenic [J]. Journal of Hazardous Materials, 2008, 153: 434–443.
- [21] DAENZER R, XU L, DOERFELT C, JIA Y, DEMOPOULOS G P. Precipitation behaviour of As(V) during neutralization of acidic Fe(II)–As(V) solutions in batch and continuous modes [J]. Hydrometallurgy, 2014, 146: 40–47.
- [22] MIN Xiao-bo, LIAO Ying-ping, CHAI Li-yuan, YANG Zhi-hui, XIONG Shan, LIU Lin, LI Qing-zhu. Removal and stabilization of arsenic from anode slime by forming crystal scorodite [J]. Transactions of Nonferrous Metals Society of China, 2015, 25: 1298–1306.
- [23] CHAI Li-yuan, YUE Meng-qing, YANG Jin-qin, WANG Qing-wei, LI Qing-zhu, LIU Hui. Formation of tooeleite and the role of direct removal of As(III) from high-arsenic acid wastewater [J]. Journal of Hazardous Materials, 2016, 320: 620–627.
- [24] LIU Jing, CHENG Hong-fei, FROST R L, DONG Fa-qing. The mineral tooeleite $\text{Fe}_6(\text{AsO}_3)_4\text{SO}_4(\text{OH})_4\cdot 4\text{H}_2\text{O}$: An infrared and Raman spectroscopic study–environmental implications for arsenic remediation [J]. Spectrochimica Acta (Part A): Molecular and Biomolecular Spectroscopy, 2013, 103: 272–275.
- [25] VIÑALS J, SUNYER A, MOLERA P, CRUELLES M, LLORCA N. Arsenic stabilization of calcium arsenate waste by hydrothermal precipitation of arsenical natroalunite [J]. Hydrometallurgy, 2010, 104: 247–259.
- [26] SUNYER A, CURRUBÍ M, VIÑALS J. Arsenic immobilization as alunite-type phases: The arsenate substitution in alunite and hydronium alunite [J]. Journal of Hazardous Materials, 2013, 261: 559–569.
- [27] BLUTEAU M, DEMOPOULOS G P. The incongruent dissolution of scorodite: Solubility, kinetics and mechanism [J]. Hydrometallurgy, 2007, 87: 163–177.
- [28] YANG Jin-qin, LI Qing-zhu, CHAI Li-yuan, WANG Qing-wei, LIU Hui, MIN Xiao-bo, XIAO Rui-yang. A new mixed-valent iron arsenate black crystal [J]. Transactions of Nonferrous Metals Society of China, 2018, 28: 1036–1044.
- [29] DRAHOTA P, FILIPPI M. Secondary arsenic minerals in the environment: A review [J]. Environment International, 2009, 35: 1243–1255.
- [30] DARBAN A K, AAZAMI M, MELÉNDEZ A M, ABDOLLAHY M, GONZALEZ I. Electrochemical study of orpiment (As_2S_3) dissolution in a NaOH solution [J]. Hydrometallurgy, 2011, 105: 296–303.
- [31] FLOROIU R M, DAVIS A P, TORRENTS A. Kinetics and mechanism of $\text{As}_2\text{S}_3(\text{am})$ dissolution under N_2 [J]. Environmental Science & Technology, 2004, 38: 1031–1037.
- [32] GUO Li, DU Ya-guang, YI Qiu-shi, LI Dun-shun, CAO Long-wen, DU Dong-yun. Efficient removal of arsenic from “dirty acid” wastewater by using a novel immersed multi-start distributor for sulphide feeding [J]. Separation and Purification Technology, 2015, 142: 209–214.
- [33] SANZ E, VEGA C, ABASCAL J L F, MACDOWELL L G. Phase

- diagram of water from computer simulation [J]. Physical review letters, 2004, 92: 255701.
- [34] LENGKE M F, TEMPEL R N. Geochemical modeling of arsenic sulfide oxidation kinetics in a mining environment [J]. Geochimica et Cosmochimica Acta, 2005, 69: 341–356.
- [35] POKROVSKI G, GOUT R, SCHOTT J, ZOTOV A, HARRICHOURY J. Thermodynamic properties and stoichiometry of As(III) hydroxide complexes at hydrothermal conditions [J]. Geochimica et Cosmochimica Acta, 1996, 60: 737–749.
- [36] TANG Bo, ZHUO Lin-hai, GE Jie-chao, NIU Jin-ye, SHI Zhi-qiang. Hydrothermal synthesis of ultralong and single-crystalline Cd(OH)₂ nanowires using alkali salts as mineralizers [J]. Inorganic Chemistry, 2005, 44: 2568–2569.
- [37] SUN Yong-gang, YAO Qi, ZHANG Xin, YANG Hong-ling, LI Na, ZHANG Zhong-shen, HAO Zhen-ping. Insight into mineralizer modified and tailored scorodite crystal characteristics and leachability for arsenic-rich smelter wastewater stabilization [J]. RSC Advances, 2018, 8: 19560–19569.

采用硫化沉淀法从酸性废水中除砷及其水热成矿稳定化

胡斌^{1,2}, 杨天足^{1,2}, 刘伟锋^{1,2}, 张杜超^{1,2}, 陈霖^{1,2}

1. 中南大学 冶金与环境学院, 长沙 410083;
2. 难治有色金属资源高效利用国家工程实验室, 长沙 410083

摘要: 为实现对含砷酸性废水的安全处理, 本文作者提出硫化法沉砷和水热成矿稳定砷的新工艺。在硫化沉淀最佳条件下, 废水中 99.65% 的砷以无定形 As₂S₃ 的形式沉淀。由于该沉淀在 TCLP 试验中砷的浸出浓度高达 212.97 mg/L, 因此, 采用水热成矿法提高 As₂S₃ 的稳定性。结果表明, 经矿化的 As₂S₃ 的砷浸出浓度仅为 4.82 mg/L。此外, 在矿化剂 Na₂SO₄ 的作用下, 无定形 As₂S₃ 可转变为 As₂S₃ 晶体, 且砷浸出液浓度进一步降至 3.86 mg/L。水热成矿法是稳定硫化砷的有效方法。因此, 该工艺在含砷废水的处理中具有较大应用前景。

关键词: 含砷废水; 除砷; 稳定化; 硫化沉淀; 水热成矿; 水热晶化

(Edited by Wei-ping CHEN)